



Seismic Response of RC Frame with Stiffness Irregularity Under Sequential Loading of Main Shock and Repeated Aftershocks

Athar Tauheed¹(✉) and Mehtab Alam²

¹ Department of Civil Engineering, Jamia Millia Islamia, Jamia Nagar, New Delhi 110025, India
athar.dce@gmail.com

² Department of Civil Engineering, Netaji Subhas University of Technology (West Campus),
New Delhi, Delhi 110073, India
mehtab.alam@nsut.ac.in

Abstract. Recorded data of seismic active regions reveal that most of the earthquake events consist of main shock succeeded by a number of aftershocks. The present code focuses on single earthquake event ignoring the possibility of following consecutive events. The structures designed for single event of earthquake lying in the earthquake prone areas may be severely damaged by main shock and repeating aftershocks. The aftershocks that accompany the main shock take their toll on the seismic demands of the buildings which goes on increasing in each successive event as the building may not be retrofitted or strengthened due to time constraint or some other reason. Along the height of the structure, the irregularity in the distribution of stiffness, mass and strength contribute to the poor performance of the buildings. The current study focuses on the consequences of seismic demands of 11-storey moment-resisting frames with peak ground acceleration 0.36g, 0.40g and 0.45g. The aftershocks considered are of two third of PGA of the main shock. Stiffness irregularity is introduced from considerations of stilt and service floor requirements in the first, second, sixth and top storey. The irregularity has been incorporated reducing the stiffness by 43% and then by 65% at the same storey level. A nonlinear dynamic analysis is carried out on the designed frame that is exposed to time history which is compatible with IS1893:2016. Seismic response has been discussed and compared with response of the main shock.

Keywords: Aftershock · Stiffness irregularity · Seismic demand · Moment resisting frame

1 Introduction

To satisfy the functional requirement of a building and at times due to architectural interference, it is not possible to maintain symmetry and uniformity in structural elements of building. A vertically irregular structure is described as one that has a non-uniform stiffness, strength, and mass along its height. Most of the buildings carry one or more irregularities. To meet out high demands of parking, ground floors are provided for the parking, where some floors are used for meeting halls, showrooms, banking halls, and

upper floors for services. This leads to stiffness and mass irregularity that is introduced by change in storey height and difference in infill walls along the height of the building. Two of the most destructive events that a building structure could experience are earthquake and blast. In designing a building structure to resist the forces induced by an earthquake, both the local response at the element level and the global response are considered. However, despite the similarities between seismic excitation and extreme loading, the global response of buildings to extreme dynamic loadings (blast and impact) is usually not considered as being critical (Ahmadi et al. 2021; Anas et al. 2020a, 2020b, 2020c; Anas et al. 2021a, 2021b, 2021c, 2021d, 2021e, 2021f, 2021g, 2021h; Anas and Alam 2022a, 2022b, 2022c; Anas et al. 2022a, 2022b, 2022c, 2022d, 2022e, 2022f, 2022g, 2022h, 2022i; Shariq et al. 2022; Tahzeeb et al. 2022a, 2022b, 2022c; Ul Ain et al. 2021; Ul Ain et al. 2022).

Basically, the irregularities are classified into two groups – vertical irregularity and plan irregularity. In this study, we are considering vertical irregularity, where the stiffness is changed for a particular storey. Irregularities develop vulnerable weak planes of higher stresses under earthquake loads. These further trigger the deterioration in stiffness and strength of a structure that may even lead to the collapse.

In general, the researchers talk about the main shock and its first aftershock in the case of regular buildings. They have ignored the significance of subsequent aftershocks. During earthquakes, the presence of irregularities enhances the vulnerability of structures which becomes a crucial parameter when sequential earthquakes hit such structures. In the present study, two stiffness irregularities have been considered. Frame with irregularities reducing stiffness by 43% (S1) and by 65% (S2) at different storeys have been taken for analysis. The storeys considered for stiffness irregularity are first, second, sixth and top one. The aim of the present research is to study the seismic response of structures with the introduced irregularity at different storey levels and comparison with corresponding regular one under the exposure of repetitive earthquakes as aftershocks with small time interval, in extreme seismic zone V of IS 1893 (Part1):2016.

As per the past studies, ample research had been done on the seismic behavior of the structures of all degrees of freedom exposed to repeated ground motions. Parekar *et al.* (2020) studied the disastrous effects of sequential earthquakes on buildings that were located in earthquake-prone areas having little time left for rehabilitation after the main-shock. It was found that the aftershocks were fatal for the buildings. They evaluated the seismic demands in terms of IDR for 3-, 6-, and 9- storey SMRF structures and examined the consequences of repetitive ground motions on them. It was concluded that there was a unusual influence on these irregular structures especially due to the aftershocks. Higher seismic demand was reported with irregularity at bottom than it was in other storeys. Oyguc et al. (2018) investigated the three plan asymmetric RC structures that had been subjected to the powerful Tohoku seismic sequences taking into consideration the performance of the structures. An inference drawn stated that in the case of irregular RC buildings, there was an increase in the residual drift demands due to the structural irregularity as compared to regular RC structures.

Loulelis et al. (2012) conducted an extensive study to investigate the seismic performance of SMRF when exposed to repeated ground motions. It was inferred that the damages as well as ductility demands of the structures was higher for the repeated ground motion against single event of earthquake. Faisal et al. (2013) carried out an extensive

study on the ductility demands of three dimensional inelastic concrete frames of 3-, 6-, 9-, 12- storeys taking into consideration the effects of multiple ground motions and concluded that it increased remarkably in the case of repetitive earthquakes. Hatzivassiliou *et al.* (2015) carried out a comprehensive study on four structures (2- regular and 2-irregular) keeping in mind the inelastic response of structures to repeated shocks against a single main shock. They deduced that the sequential earthquakes increased seismic demands which augmented ductility demand parameter of the buildings. Raghunandan *et al.* (2015) investigated the chances of collapse of the RC frame buildings and concluded with dimmed chances of survival if the damage resulting due to main shock was significantly high. Damage indicators were used to calculate the possibility of collapse of the structure amongst which the best damage measure was the drift caused in the structure.

Hatzigeorgiou (2010) devised a new method to study the ductility demands of the SDOF systems under the influence of sequential ground motions. The force reduction factor was considered as a parameter to achieve both cumulative damages as well as ductility demands of the structure. It was concluded that the design earthquake lead to less conservative force reduction factors as against a series of earthquakes. Goda (2012) studied the ductility demand of inelastic SDOF systems and examined the consequences of aftershocks with the help of real and artificial seismic sequences. A similarity was observed in the ductility demands of both real and artificial sequences which implied that the latter could be used as a substitute for the real ones. Hosseinpour *et al.* (2017) had studied both regular and irregular eight storeyed structures to investigate the fragility curves for them under the effect of multiple earthquakes. A conclusion was drawn that the regular building lesser vulnerability under the influence of aftershock as compared to the irregular ones.

In this study, seismic demand of a 11storey frame without any irregularity, T_0 frame, is compared with corresponding frames having stiffness irregularity in the first $T_{1,1}$ & $T_{2,1}$, second $T_{1,2}$ & $T_{2,2}$, sixth $T_{1,3}$ & $T_{2,3}$, and top $T_{1,4}$ & $T_{2,4}$ storey as shown in Table 1 subjected to synthetically prepared main shock and its subsequent aftershocks compatible with design response spectrum available in IS 1893(Part1):2016.

2 Description of the Structure

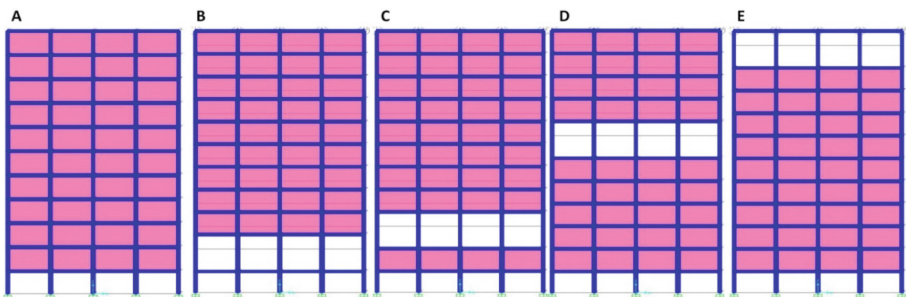


Fig. 1. Elevation detail of 11storey RC frames regular A (T_0); Stiffness Irregularity in first storey B ($T_{1,1}/T_{2,1}$), second storey C ($T_{1,2}/T_{2,2}$), sixth storey D ($T_{1,3}/T_{2,3}$), and top storey E ($T_{1,4}/T_{2,4}$).

Table 1. Types of frames

T ₀	Without Stiffness irregularity (Regular)
T _{1,1}	Reducing stiffness by 43% in First storey (S1)
T _{1,2}	Reducing stiffness by 43% in Second storey (S1)
T _{1,3}	Reducing stiffness by 43% in Six storey (S1)
T _{1,4}	Reducing stiffness by 43% in Top storey (S1)
T _{2,1}	Reducing stiffness by 65% in First storey (S2)
T _{2,2}	Reducing stiffness by 65% in Second storey (S2)
T _{2,3}	Reducing stiffness by 65% in Six storey (S2)
T _{2,4}	Reducing stiffness by 65% in Top storey (S2)

An RCC building with symmetric plan consisting of five columns located at five meter each bay and 3.2 m storey height as shown in Fig. 1, has been chosen in this study. Intermediate frame of the building is selected for seismic analysis. The building is assumed to be located in the zone V as per IS1893: (Part1):2016. SAP2016, commercial software has been used to model the geometry and performing the analysis and design. Assumed load data are: self-weight of the slab including floor finishing –12.5 kN/m, floor live load –5 kN/m, roof live load –3.75 kN/m, self-weight of partition wall –7.5 kN/m, and earthquake load as per IS1893. All the columns of size 450 mm × 450 mm, and all beams are of overall size 230 mm × 450 mm. Concrete is of grade M25 for all the members. Main steel reinforcement is of grade Fe500, while transverse steel is of grade Fe415. Park model for stress-strain response for steel re-bar, and Mander material model to characterize the confined concrete are used.

Building frame T₀ with stiffness irregularity in the first, second, sixth, and tenth storey having one at a time is incorporated. In this study, nine models of the frames have been considered out of which only one is regular (T₀) as shown in Fig. 1. Stiffness irregularity is introduced one at a time at first (T_{1,1})/second (T_{1,2})/sixth (T_{1,3})/top storey (T_{1,4}), by increasing the height from 3.2 m to 3.85 m, or reducing the stiffness by 43% as depicted in Fig. 1(B, C, D, E). In the rest of the models, stiffness irregularity is introduced by incrementing the height from 3.2 m to 4.5 m, or reducing the stiffness by 65% at the same locations as that in earlier ones that are first (T_{2,1})/second (T_{2,2})/sixth (T_{2,3})/top storey (T_{2,4}) as depicted in Fig. 1(B, C, D, E) as per Table 1. Nonlinear time-history analyses of the building frames are performed for scaled ground acceleration time histories which are compatible with IS1893:2016 corresponding to 0.36g, 0.40g and 0.45g PGAs as main shocks by making use of software SAP2000.

3 Sequential Ground Motion

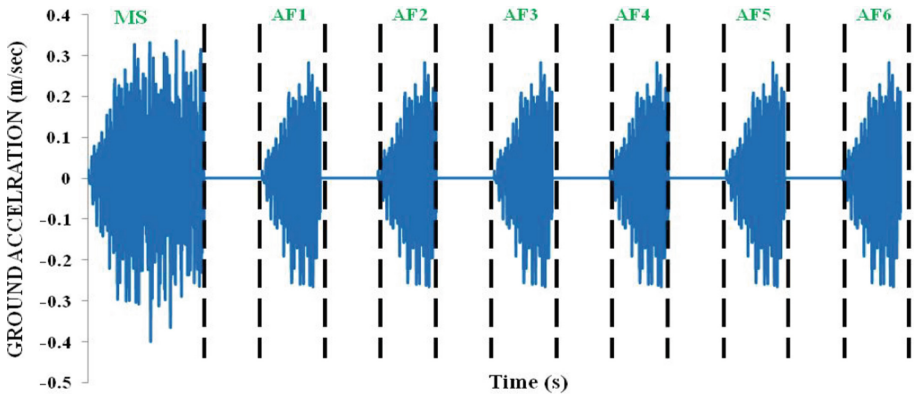


Fig. 2. Considered Ground Acceleration-Time, compatible to IS 1893:2016.

Table 2. Sequential ground motion

Case 1	0.36g PGA as main shock & six aftershocks
Case 2	0.40g PGA as main shock & six aftershocks
Case 3	0.45g PGA as main shock & six aftershocks

The main shock accompanied with its six aftershocks with acronyms MS, 1AS, 2AS, 3AS, 4AS, 5AS, 6AS respectively form sequential ground motion compatible with the response spectrum (IS1893:2016) are the inputs. Main shock (30 s) and six aftershocks (15 s) are sequentially joined one after another to form the sequence of earthquake events. The time-history is scaled to three peak accelerations of PGAs (0.36g (Case-1), 0.4g (Case-2), and 0.45g (Case-3) are taken as main shocks. Each aftershock is assigned with PGA of two-third of its main shock PGA as shown in Table 2. Between two consecutive shocks of a sequential ground motion input, acceleration zero amplitude with time-lapse of 100 s has been inserted to ensure the structure comes to rest as shown in Fig. 2.

4 Result and Discussions

4.1 Seismic Behaviour of the Frames

Eight irregular frames (4 for S1, 4 for S2) having stiffness irregularity at different storeys along with a regular frame as shown in Fig. 1A are taken into account to carry out the non-linear dynamic analysis under the repetitive earthquakes of varying magnitudes with PGAs as 0.36g, 0.4g and 0.45g. Each of the main shocks is followed by its six aftershocks

and is two-third of the PGA of each. Comparative analyses of the response of regular frames with each irregular frame subjected to the same sequential loading and loading with higher PGA are carried out keeping an eye on the following parameters.

4.2 Maximum Horizontal Top Floor Displacements

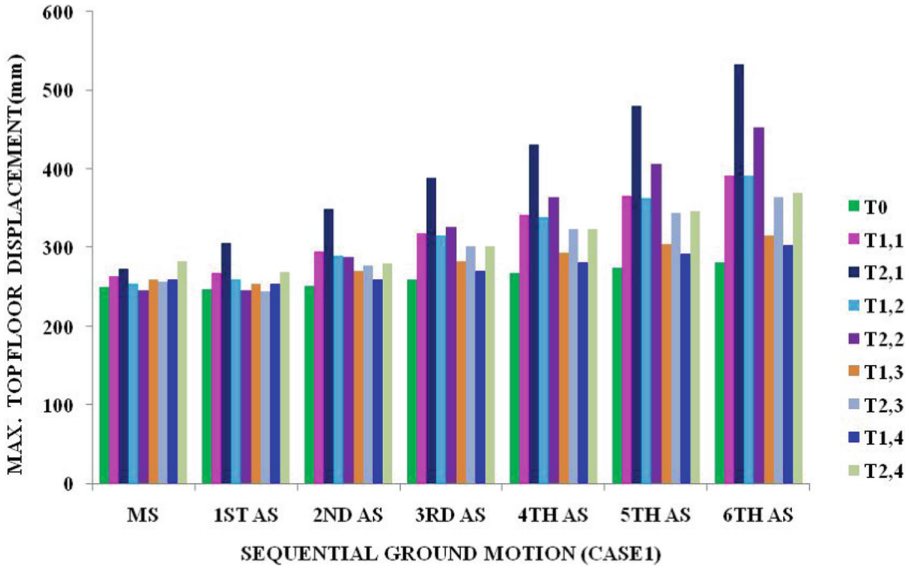


Fig. 3. Maximum top storey displacements (Case 1).

Results obtained for maximum top floor transient displacements for different frames subjected to main shock of peak ground acceleration 0.36g, 0.4g, 0.45g and their respective six aftershocks from analyses are plotted in Figs. 3, 4, and 5. It is observed that the maximum top horizontal displacement consistently increases with the number of aftershocks. Since aftershock has less intensity as compared to its main shock, it is expected to have less maximum top story displacement in the aftershock if it would have started with zero initial condition. However, the oscillation in the aftershock starts with a residual displacement and therefore, the maximum top story displacement in the aftershock depends on the value of the initial displacement.

The regular frames (T_0) as well as **S1** ($T_{1,1}$ to $T_{1,4}$), survive with the main shocks of PGAs 0.36g (**Case1**) and 0.40g (**Case2**) and their aftershocks. It is observed that the value of top floor displacement for $T_{1,1}$; $T_{1,2}$; $T_{1,3}$, and $T_{1,4}$ during the main shock as well as the aftershocks, is greater than T_0 . However, studying the response during aftershocks in this case, the value decreases in the first aftershock of T_0 , $T_{1,3}$, and $T_{1,4}$ but increases in $T_{1,1}$ and $T_{1,2}$. It is observed that the increment in displacement values during all the aftershocks in each of the types is gradual. A holistic view of **Case 1** exhibits that the values of top floor displacement for $T_{1,1}$, and $T_{1,2}$ have a similar trend for the

displacement under the main shock and aftershocks and are higher as compared to the other types as shown in Fig. 3.

For **S2** (Type $T_{2,1}$ to Type $T_{2,4}$), all the frames survive with the main shock of 0.36g and its aftershocks in **Case 1**. It is seen that the value of top floor displacement for the frames $T_{2,1}$; $T_{2,3}$, and $T_{2,4}$ during the main shock is greater than the frame T_0 , but frame $T_{2,2}$ exhibits slightly lesser value of the displacement. However, during the aftershocks in this case, the value decreases in the first aftershock of the frames T_0 ; $T_{2,3}$, and $T_{2,4}$ but increases in $T_{2,1}$, and $T_{2,2}$. It is observed that the increment in displacement values during all the aftershocks is gradual unlike in $T_{2,1}$ where the increase is steep. Despite having a lower value in main shock, $T_{2,2}$ shows a steep trend in the values but lesser than $T_{2,1}$ during its aftershocks. The displacement values for the frames $T_{2,3}$ and $T_{2,4}$ during the aftershocks also show a higher gradual increase as compared to the frame T_0 .

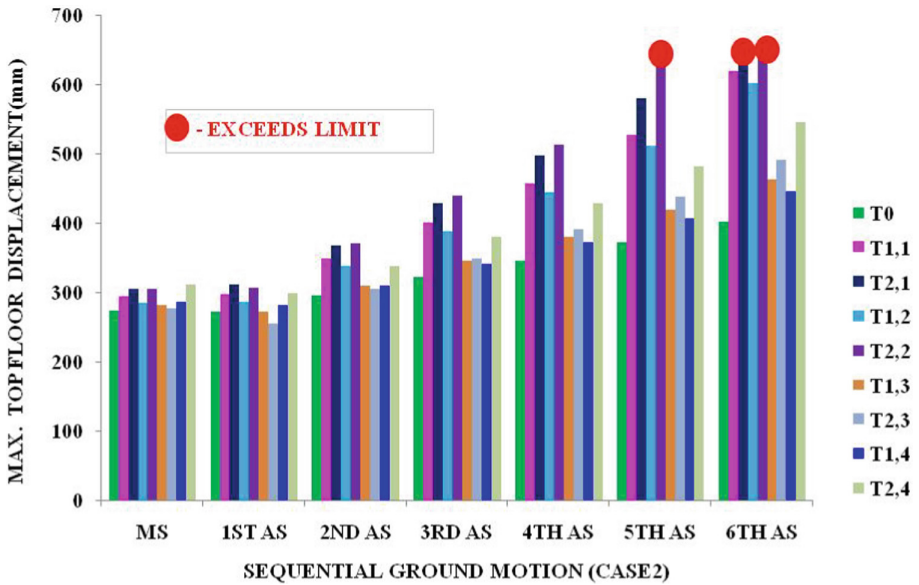


Fig. 4. Maximum top floor displacements (Case 2).

For the frames subjected to 0.4g PGA and its aftershocks i.e., **Case 2** with irregularity **S1**, it is observed that the value of top floor displacement for the frames $T_{1,1}$; $T_{1,2}$, $T_{1,3}$, and $T_{1,4}$ during the main shock as well as the aftershocks is greater than the frame T_0 . However, studying the aftershocks in this case, the displacement decreases in the first aftershock of the frames T_0 ; $T_{1,3}$, and $T_{1,4}$ but increases in the frames $T_{1,1}$ and $T_{1,2}$. It is observed that increment in the displacement values during all the aftershocks in frames T_0 ; $T_{1,3}$, and $T_{1,4}$ is gradual but becomes steep in frames $T_{1,1}$, and $T_{1,2}$. A comprehensive comparison of the displacement values of case 2 exhibits the values of top floor displacement for $T_{1,1}$ and $T_{1,2}$ have a similar trend in the displacement values during main shock and aftershocks and are higher as compared to the other types as per Fig. 4.

Now for stiffness irregularity **S2**, it is seen that the value of top floor displacement of the frames $T_{2,1}$; $T_{2,2}$; $T_{2,3}$, and $T_{2,4}$ during main shock is greater than the frame T_0 . However, the value decreases during the first aftershock of the frames T_0 ; $T_{2,3}$, and $T_{2,4}$ but increases in the frames $T_{2,1}$ and $T_{2,2}$. During every aftershock in frames $T_{2,1}$ and $T_{2,2}$, the increment in the values is sharp which makes the frame to fail in the last and fifth aftershocks. There is a slower increase in the displacement values of the frames $T_{2,3}$, and $T_{2,4}$ but the top floor displacement attains a higher value in the frame $T_{2,4}$ than in the frames T_0 , and $T_{2,3}$. Subsequently, the frames of T_0 , $T_{2,3}$, and $T_{2,4}$ survive with the main shock and their respective aftershocks as can be seen in Fig. 4.

Under the sequential ground motion of 0.45g PGA and its aftershocks i.e., **Case 3**, the top floor displacement of the frames with stiffness irregularity **S1**, it is seen that the value of top floor displacement of the frames $T_{1,1}$; $T_{1,2}$; $T_{1,3}$, and $T_{1,4}$ during main shock is greater than T_0 . However, the value decreases in the first aftershock of T_0 , $T_{1,2}$, $T_{1,3}$, and $T_{1,4}$ but increases in $T_{1,2}$. There is a steep rise in the values of top floor displacement in all five types after the first aftershock. The T_0 frame survives with the main shock of 0.45g PGA and its subsequent aftershocks but fails to survive in the end aftershock. During each of the aftershocks, the frames $T_{1,1}$ and $T_{1,2}$ undergo sharp increment of the displacement leading to the failure of the frames in the fourth and fifth aftershocks. $T_{1,3}$ and $T_{1,4}$ frames also withstand the main shock of 0.45g PGA and its four successive aftershocks but fail to survive with the fifth one as depicted in Fig. 5.

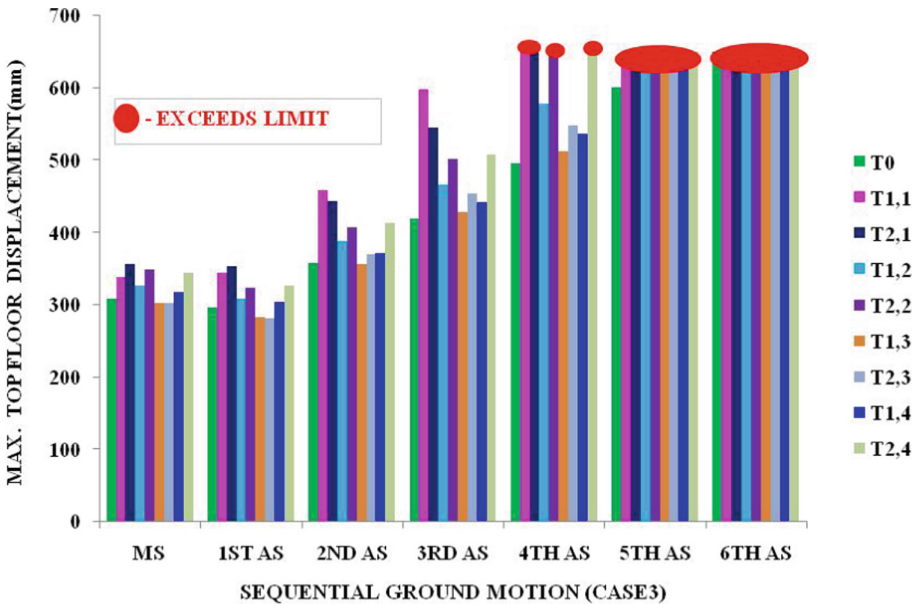


Fig. 5. Maximum top floor displacements (Case 3).

In the frames with irregularity **S2**, it is seen that the value of top floor displacement for $T_{2,1}$, $T_{2,2}$, and $T_{2,4}$ during main shock is greater than T_0 but the value of the displacement in $T_{2,3}$ is slightly less than T_0 . Also studying the results under the aftershocks in this case,

the displacement decreases in the first in all the frames as compared to the main shock. There is a steep rise in the values of top floor displacement in all five types after the first aftershock. The T_0 frame survives the main shock of 0.45g PGA and its succeeding aftershocks up to fifth but gives in during the last one. The $T_{2,1}$, $T_{2,2}$, and $T_{2,4}$ frames also withstand the main shock of 0.45g PGA and its succeeding ones up to third but could not withstand the fourth aftershock. $T_{2,3}$ frame survives with the main shock and its fourth aftershock but does not survive during the fifth as given in Fig. 5.

4.3 Maximum Residual Horizontal Top Displacements

From Fig. 6 to Fig. 8, it is seen that with the increment in the number of aftershocks there is an increase in the residual top storey displacement just like the maximum top storey displacement. The reason behind the increment is the accumulation of the residual displacements occurring in consecutive aftershocks. For the residual top displacement in **case 1 for S1**, it is seen that there is a decrease in the value of main shock for $T_{1,1}$; $T_{1,2}$, and $T_{1,3}$ and increases in $T_{1,4}$ as compared to regular frame T_0 . There is an increase in the values during each subsequent aftershock in all five types, but the increase is least in the case of the regular model and highest in $T_{1,1}$. It is noticed that the values displacements in $T_{1,1}$ and $T_{1,2}$ are approximately equal to each other during the aftershocks. The value attained after the main shock in $T_{1,2}$ is lesser than $T_{1,1}$ but ultimately both achieve approximately the same value in their last aftershocks. Similar is the case of $T_{1,3}$ and $T_{1,4}$ where the values of $T_{1,3}$ and $T_{1,4}$ are approximately equal to each other during the aftershocks. The value attained after the main shock in $T_{1,3}$ is lesser than $T_{1,4}$ but eventually attain nearly the same value in their last aftershock. The trend in the increase in values is higher in $T_{1,1}$ and $T_{1,2}$ as compared to types $T_{1,3}$ and $T_{1,4}$ as depicted in Fig. 6.

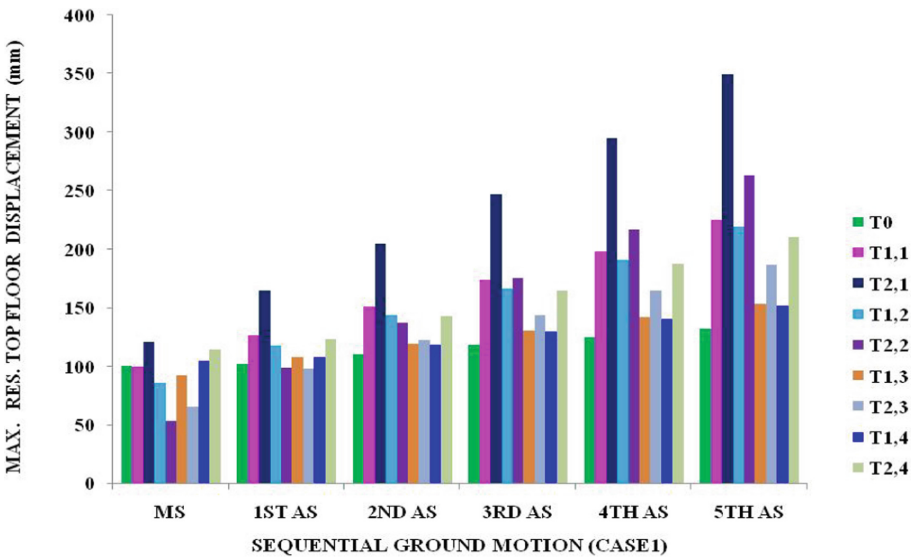


Fig. 6. Maximum residual top floor displacement (Case 1).

Now for **S2**, in the case of residual floor displacement for case1, the values of the main shock decrease for $T_{2,2}$ and $T_{2,3}$ but increases in $T_{2,1}$ and $T_{2,4}$ as compared to T_0 . There is a general incrementing trend amongst the values in all the types during the aftershocks respectively. For $T_{2,1}$, the increase in the values is the steepest in comparison to T_0 ; $T_{2,2}$; $T_{2,3}$ and $T_{2,4}$ where the increment is moderate or slow. During the last aftershock, it is noticed that the residual top floor displacement is found to be the lowest for T_0 . The value of residual displacement lies within the permissible limits for all the frames.

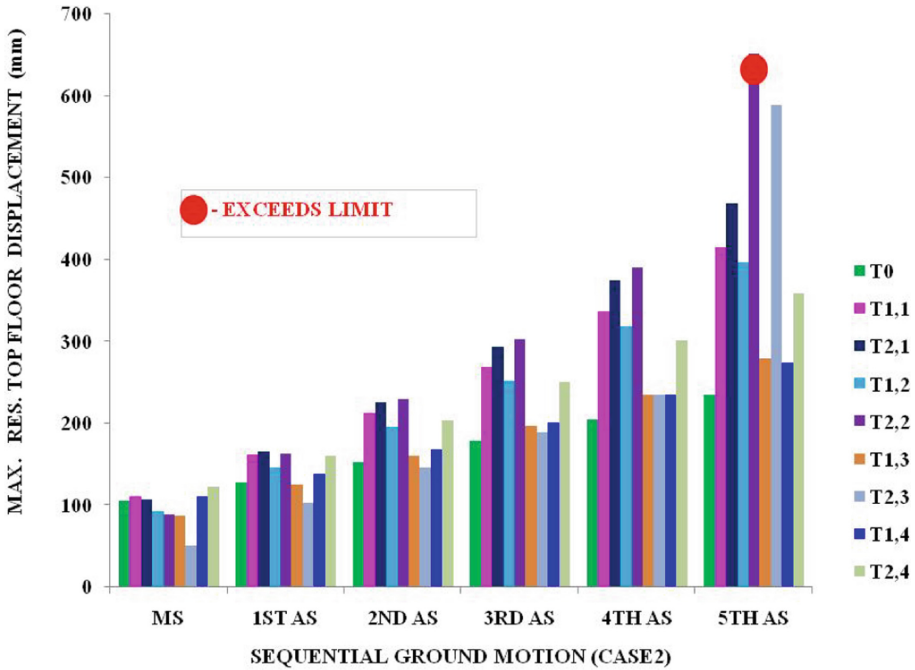


Fig. 7. Maximum residual top floor displacement (Case 2).

Coming to **case 2 for S1**, it is seen that there is a decrease in the value of main shock for types 3 $T_{1,2}$ and 4 $T_{2,3}$ and an increase in $T_{1,1}$, and $T_{1,4}$ as compared to T_0 . There is a steep rise in each of the values of the successive aftershocks in $T_{1,1}$, and $T_{1,2}$, but moderate in $T_{1,3}$ and $T_{1,4}$ and slowest in T_0 . The steepest increase is seen in $T_{1,1}$ amongst all. It is noticed that the values of $T_{1,3}$ and $T_{1,4}$ are approximately equal to each other during the aftershocks. The value attained after the main shock in $T_{1,3}$ is lesser than $T_{1,4}$ but ultimately $T_{1,3}$ attains a higher value in comparison to $T_{1,4}$ in their last aftershocks. For both the cases that are **Case 1** and **Case 2**, the building frames survive with the main shock, and its aftershocks as seen in Fig. 7.

For **S2 in Case 2**, the residual floor displacement for the values of the main shock decreases for $T_{2,2}$ and $T_{2,3}$ but increases in $T_{2,1}$ and $T_{2,4}$ as compared to T_0 . The values go on increasing in all the types during the aftershocks respectively. For $T_{2,1}$ and $T_{2,2}$, the increase in the values is the steepest followed by type $T_{2,4}$ where the increase is

moderately preceded by $T_{2,3}$ and T_0 . During the last aftershock, it is noticed that the residual top floor displacement is found to be the lowest for T_0 . The value of residual displacement lies within the permissible limits for all the frames except $T_{2,2}$ which exceeds the limit during the fifth aftershock.

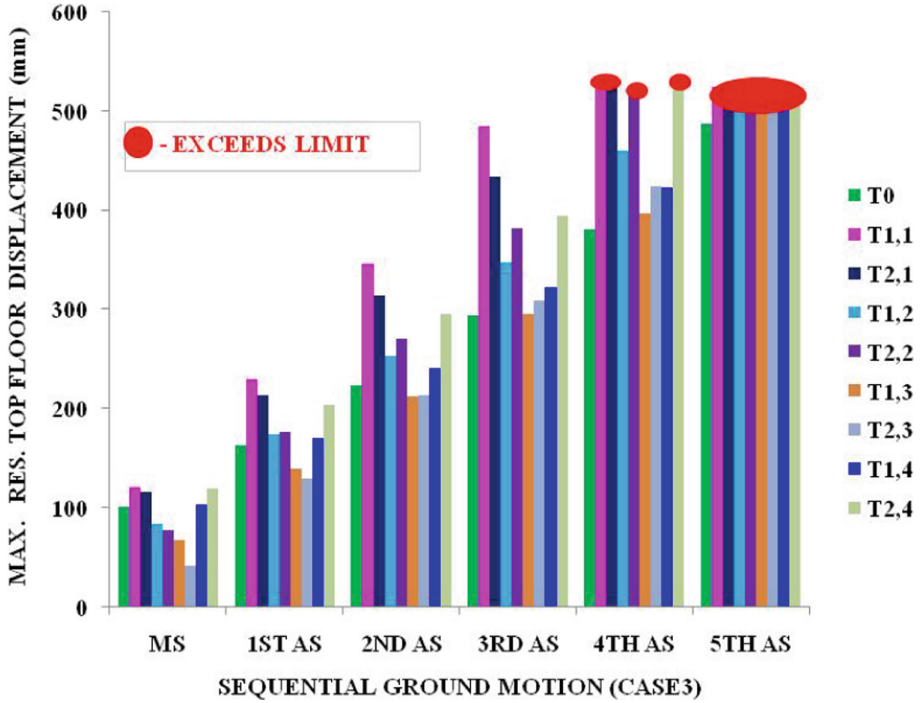


Fig. 8. Maximum residual top floor displacement motion (Case 3).

In case 3 for S1, it is observed that there is a decrement in the value of main shock for $T_{1,2}$, and $T_{1,3}$ and increment in $T_{1,1}$, and $T_{1,4}$ as compared to T_0 . There is a steep rise in each of the values of the successive aftershocks in all the types. The steepest increase is seen in $T_{1,1}$ followed by $T_{1,2}$; $T_{1,4}$, and $T_{1,3}$. $T_{1,1}$ fails at the earliest amongst all in the fourth aftershock, whereas types $T_{1,2}$; $T_{1,3}$, and $T_{1,4}$ fail during the fifth aftershock but T_0 survives as exhibited in Fig. 8.

For S2, it is observed that in Case 3, the value of residual floor displacement during main shock decreases for $T_{2,2}$ and $T_{2,3}$ but increases in $T_{2,1}$, and $T_{2,4}$ as compared to T_0 . During every aftershock in each type the values go on increasing steeply. The residual floor displacement of only T_0 frame stays within the permissible limit during the main shock and its aftershocks. The displacements of the frames $T_{2,1}$; $T_{2,2}$, and $T_{2,4}$ exceed the permissible limit during their fourth aftershock whereas $T_{2,3}$ does so in the fifth aftershock.

4.4 Maximum Storey Drift

Figures 9, 10, and 11 exhibits the maximum storey drift at each aftershock that follows the main shock. It is observed that with the increase in the number of aftershocks there is an increment in the storey drift. The reason behind the increase for the increment of storey drift is the same as that is found for top storey displacement with every consecutive aftershock. Regular shifting of storey drift from one storey to the other is observed amongst all the cases in their respective main shocks which are followed by aftershocks. The value of the storey drift goes on increasing for each type and the lowest is recorded in the case of the regular frame.

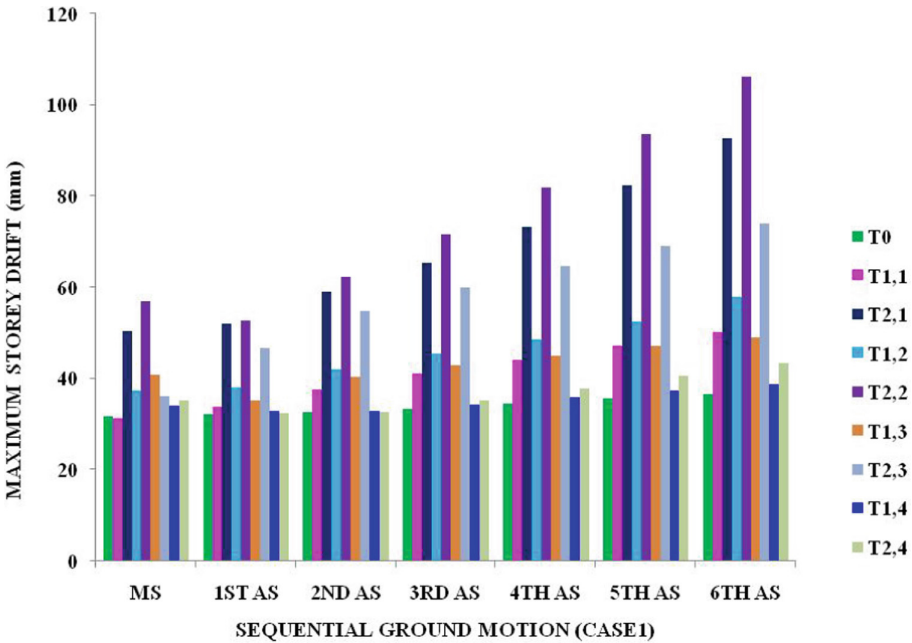


Fig. 9. Maximum storey drift (Case 1).

In Case 1 (T_0), maximum storey drift during main shock is in 6th storey shuffles to 3rd and 4th storey in the first and second aftershock and remains in the same storey for the subsequent aftershocks. For S1 ($T_{1,2}$), it is found that the drift is in the 3rd storey for the main shock and its two successive aftershocks. It shifts to the 4th storey for the remaining aftershocks. In $T_{1,2}$ and $T_{1,3}$ frames the drift is in the 2nd and 6th storey respectively for entire duration of Case 1. For $T_{1,4}$, drift is in the 6th storey during the main shock, shifts to the 3rd storey during the first aftershock and then shifts to the 4th storey for the next four aftershocks and finally shifts to 5th storey due to the last aftershock. A comprehensive study of the values of storey drifts attained after the last aftershock exhibits that $T_{1,2}$ has the highest value followed by $T_{1,1}$; $T_{1,3}$; $T_{1,4}$ and T_0 in succession. All the frames (T_0 to $T_{1,4}$) lie within the permissible limit in the Case1 depicted in Fig. 9.

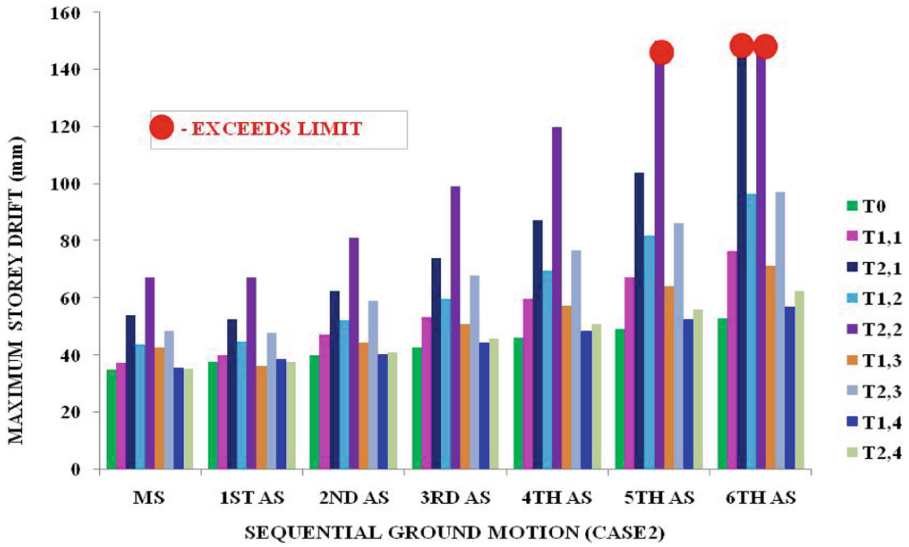


Fig. 10. Maximum storey drift (Case 2).

For **S2** irregularity in all the cases, it is seen that the storey drift keeps on travelling from one storey to another during their respective main shock and aftershocks as per Fig. 10. The drift for each type follows an incrementing order (lowest in frame T_0) during the main shock and aftershocks. For $T_{2,1}$; $T_{2,2}$, and $T_{2,3}$ frames the storey drift is found in the 1st, 2nd, and 6th storey respectively for their main shocks as well as their aftershocks.

In **Case 2** (T_0), the storey drift shifts from the 6th to 3rd storey during main shock and the first three aftershocks respectively and then to the 4th storey for the remaining aftershocks. For irregularity **S1** in $T_{1,2}$, it is noted that the storey drift is seen at the 1st storey for the main shock. It shifts to the 3rd storey in all its aftershocks. For $T_{1,2}$, the storey drift is in 2nd storey due to main shock and all its aftershocks. For $T_{1,3}$, drift is in 6th storey for the main shock and all its aftershocks. For $T_{1,4}$, the storey drift is at the 6th storey during the main shock shifts to the 3rd storey during the first aftershock and then shifts to the 4th storey for the remaining aftershocks. A holistic evaluation of the values of storey drifts achieved after the last aftershock shows that $T_{1,2}$ frame has the highest value followed by $T_{1,1}$; $T_{1,3}$; $T_{1,4}$ and T_0 in succession. All the frames (T_0 to $T_{1,4}$) lie within the permissible limits in Case2, Fig. 10.

For **S2** irregularity in $T_{2,1}$; $T_{2,7}$, and $T_{2,3}$ the storey drift is formed at the 1st, 2nd, 6th storey respectively for their main shocks and aftershocks. For $T_{2,4}$, the storey drift shifts from 6th storey during main shock to 3rd storey during the first aftershock then to 4th storey during the second and subsequent ones. A comprehensive analysis of the values of storey drifts is that after the last aftershock type 3 exceeds the limit during the fifth aftershock whereas $T_{2,1}$ does the same during its 6th aftershock. The rest of the frames stay within the permissible limit in **Case2**.

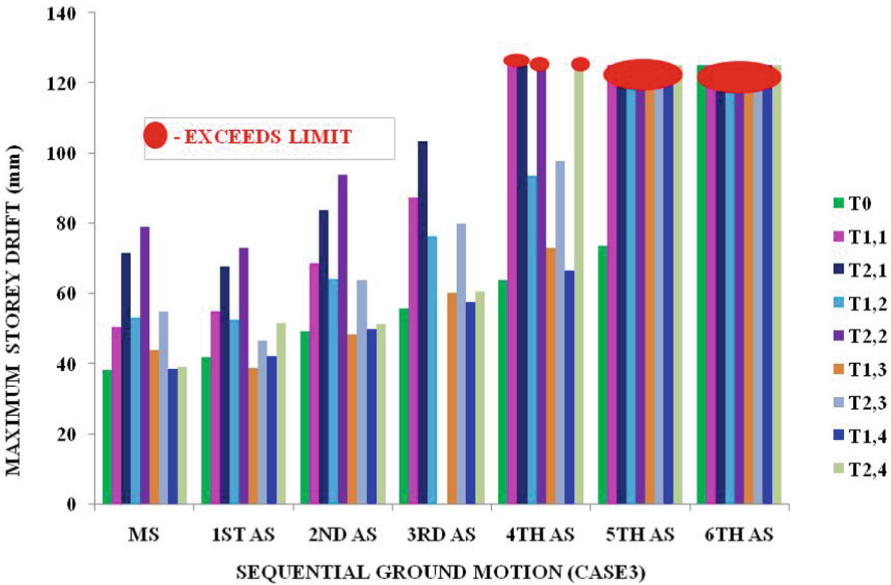


Fig. 11. Maximum storey drift (Case 3).

Examining T_0 frame under **Case3** of sequential ground motion, the drift is in 4th storey due to main shock and shuffles to 3rd storey for the remaining aftershocks and fails in the last one. For **S1** irregularity in $T_{1,1}$ frame, the storey drift is in the 1st storey after the main shock and the next three aftershocks. It exceeds the permissible limit during the fourth aftershock. For type 3 frame, it is noted that the storey drift is in 2nd storey due to main shock and the next four aftershocks. It exceeds the permissible limit during the fifth. For $T_{1,3}$, it is seen that the main shock causes storey drift in the 6th storey shuffles to the 3rd storey due to first aftershock and then to the 6th storey for the last three aftershocks. It exceeds the permissible limit during the fifth aftershock. For frame $T_{1,4}$, main shock causes the drift in 4th storey which shifts to the 3rd storey for the next three aftershocks. It exceeds the permissible limit during the fifth aftershock. The drift is relatively higher for the location of **S1** stiffness irregularity in the first, and second storey in comparison to the sixth and top storey and it is the highest with the first storey as exhibited in Fig. 11.

With **S2** irregularity in frames $T_{2,1}; T_{2,2}$ and $T_{2,3}$, the drift is formed in the 1st, 2nd, and 6th storey respectively due to main shock as well as their aftershocks. For $T_{2,1}$ and $T_{2,2}$ frames it exceeds the permissible limit in the fourth aftershock whereas $T_{2,3}$ frame fails in the fifth aftershock. For $T_{2,4}$, the drift is found in the 3rd storey due to the main shock and the first two aftershocks, then shift to the 4th storey during the third aftershock and collapses in the next aftershock as per Fig. 12. It is observed that the drift is relatively more in the case of irregularity in the first storey and the storey in comparison to the fifth and top storey and it is the highest in first storey.

Second storey is the only location of maximum storey drift coincides with the storey of **S1** irregularity under all the three cases of episodes. Maximum storey drift remains

with the storey of stiffness irregularity S2 that are first, second, and sixth under the three cases of episodes.

4.5 Maximum Residual Storey Drift

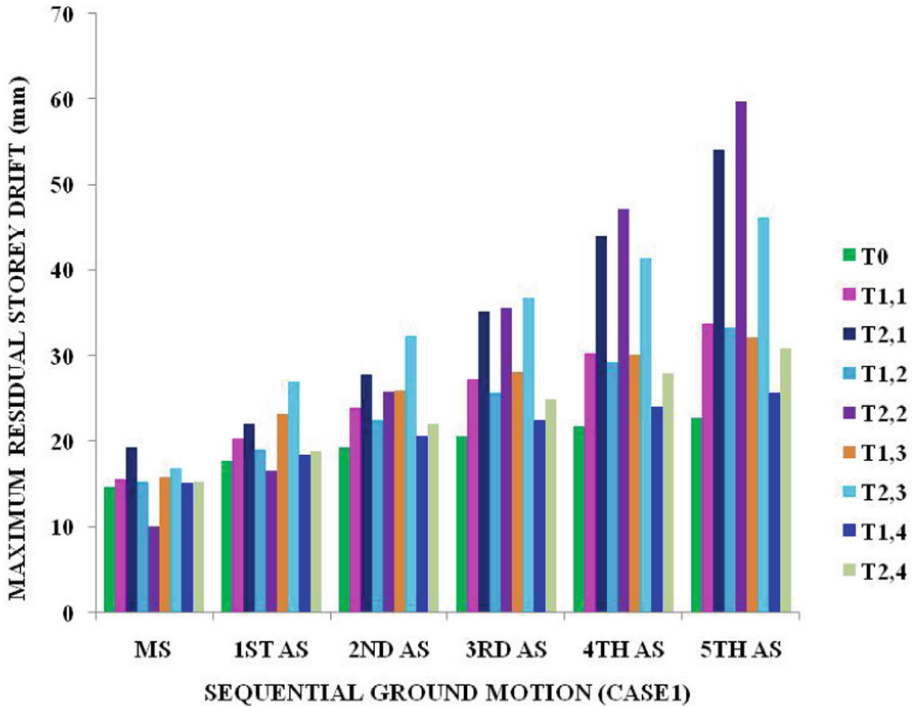


Fig. 12. Maximum residual storey drift (Case 1).

There is an increment in the maximum residual drift with the number of aftershocks. This is similar to the maximum drift as can be interpreted from the Fig. 12, 13, and 14. From the analyses results, it can be stated that the frames with irregularity considered are strong enough to bear with the episodes of 0.36g PGA and 0.4g PGA but not the episode of 0.45g PGA.

From Fig. 13, for the regular frame T₀, the residual drift lies with 7th storey due to the main shock and shuffles to 6th storey in the first aftershock and remains there for the rest of the aftershocks. For S₁ irregularity, the drift for T_{1,3} frame is the maximum during the main shock and its first three aftershocks, but in the last two aftershocks T_{1,1} frame has the maximum values. T_{1,1} frame gets the formation of maximum residual storey drift in 7th storey from main shock and shifts to 6th storey for the rest of the aftershocks. T_{1,2} frame has the maximum residual storey drift in 7th storey in the main shock and shifts to 6th storey in the first three aftershocks and then to 5th storey for the remaining ones. T_{1,3} frame has the formation of drift in the 6th storey due to main shock and all its

aftershocks. Frame T1,4 has the got it in 7th storey in the main shock, shifts to 6th storey in the first aftershock and continues to stay there for the rest. The maximum residual storey drifts is achieved due to last aftershock for all the types are T_{1,1} followed by T_{1,2}; T_{1,3}; T_{1,4}, and T₀ with descending trend.

Random shuffling of the maximum residual storey drift in the frames with S2 irregularity is also achieved post last aftershock in all the frames but having its maximum value in T_{2,2} followed by T_{2,1};T_{2,3}, and T_{2,4} with descending trend as shown in Fig. 12.

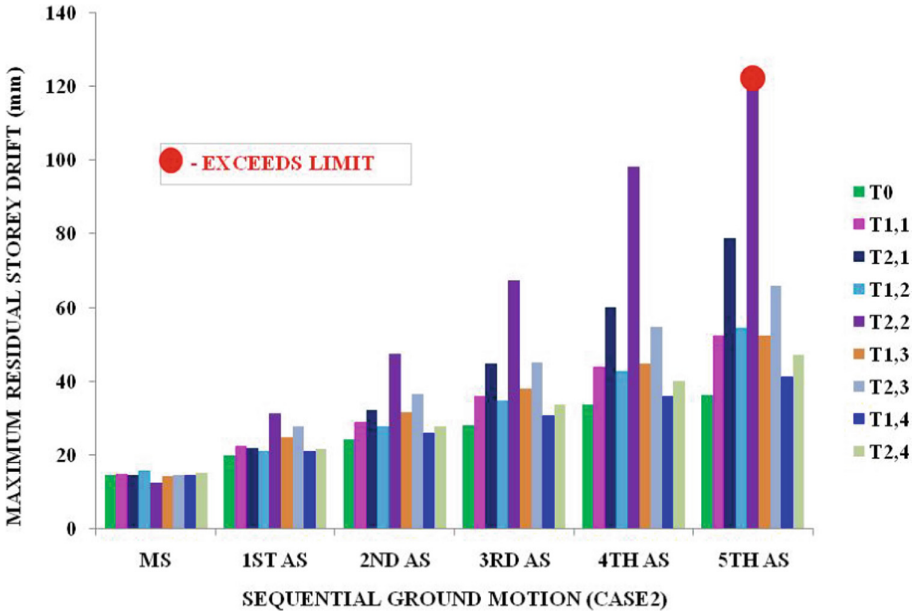


Fig. 13. Maximum residual storey drift (Case 2).

All the frames with irregularity S1 subjected to Case 2 episode, Fig. 13 shows that the maximum residual drift within permissible limit. The frame T_{1,2} attains the maximum value of the residual drift followed by the frames T_{1,3}, and T_{1,4}. The frames with stiffness S2 under episode of Case2, frame T_{2,2} only attains the maximum value exceeding the permissible value and frames T_{2,1}, T_{2,3} and T_{2,4} follow descending trend with the drift within permissible limit.

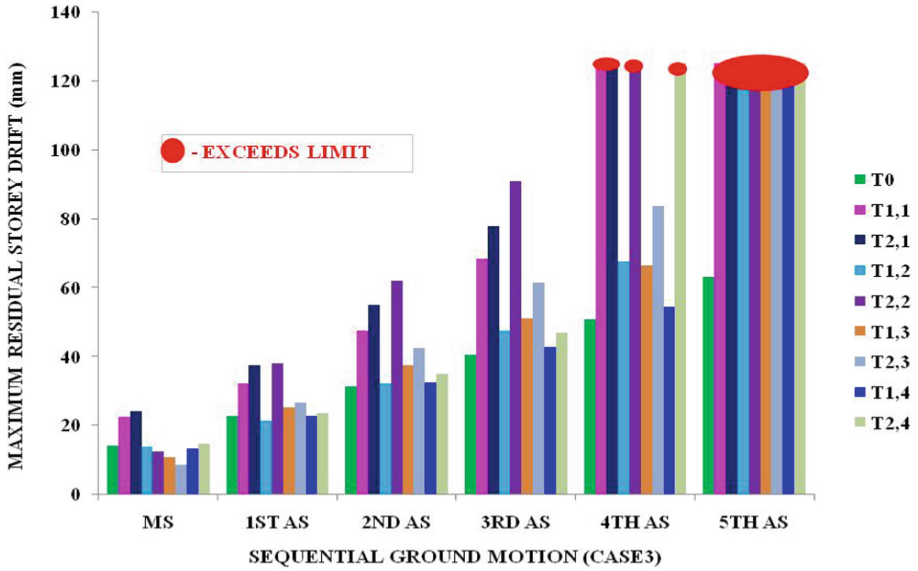


Fig. 14. Maximum residual storey drift (Case 3).

The frames with irregularity **S1** subjected to Case 3 episode, Fig. 14 shows that the frame $T_{1,1}$ fails earlier by undergoing maximum storey drift exceeding the permissible limit due to fourth aftershock while frames $T_{1,2}$; $T_{1,3}$, and $T_{1,4}$ fail under fifth aftershock. However, the frames with irregularity **S2** and subjected to episode Case3, $T_{2,1}$; $T_{2,2}$, and $T_{2,4}$ frames fail earlier by undergoing maximum storey drift exceeding the permissible limit due to fourth aftershock while frame $T_{2,3}$ survives and fails under next i.e., fifth aftershock.

4.6 Formation of Plastic Hinges

Numerous damages occur on the building frames when they are subjected to a series of earthquakes. The probable loss of strength and stiffness in the form of damages that a building frame may suffer can be predicted by keeping a track of the locations of formation of plastic hinges. Hinges formed in the frames with considered stiffness **S1** and **S2** during the sequential ground motions of PGAs 0.36g, 0.40g and 0.45g are exhibited in Figs. 15, 16 and 17, depict the total count of hinges formed and also their transformation from one state to another during the main shock and its aftershocks. The plastic rotation that takes place during the repetitive earthquakes leads to storey drift and permanent floor displacement.

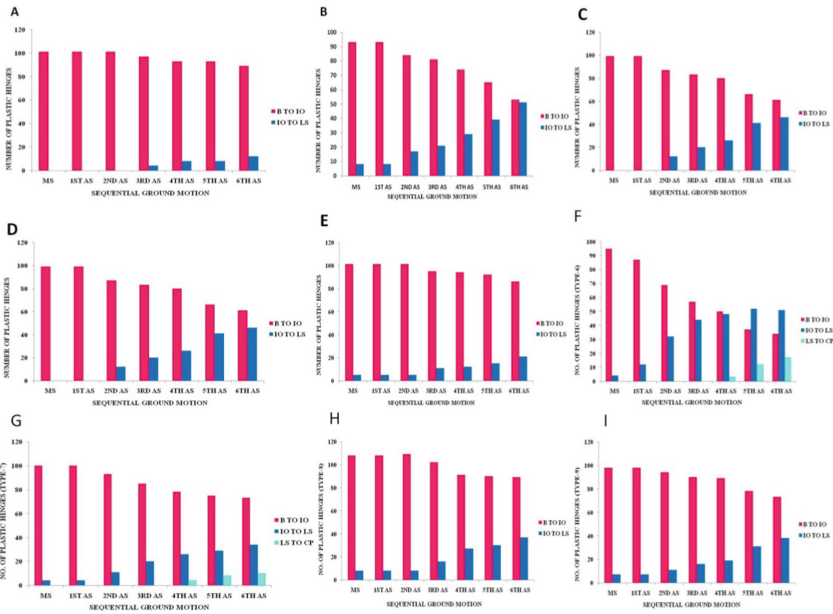


Fig. 15. Number of hinges pattern for A (T_0), B ($T_{1,1}$), C ($T_{1,2}$), D ($T_{1,3}$) and E ($T_{1,4}$), F ($T_{2,1}$), G ($T_{2,2}$), H ($T_{2,3}$), I ($T_{2,4}$) for case 1.

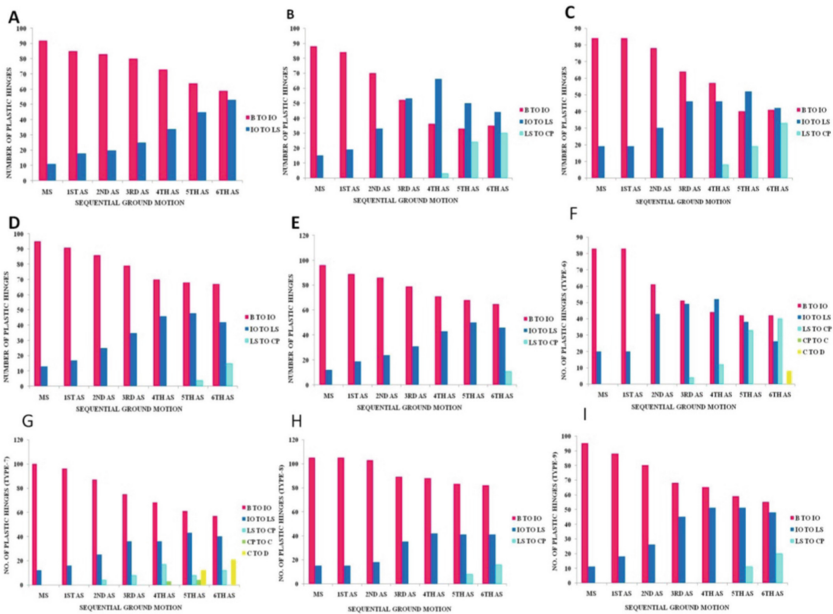


Fig. 16. Number of hinges pattern for A (T_0), B ($T_{1,1}$), C ($T_{1,2}$), D ($T_{1,3}$) and E ($T_{1,4}$), F ($T_{2,1}$), G ($T_{2,2}$), H ($T_{2,3}$), I ($T_{2,4}$) for case 2.

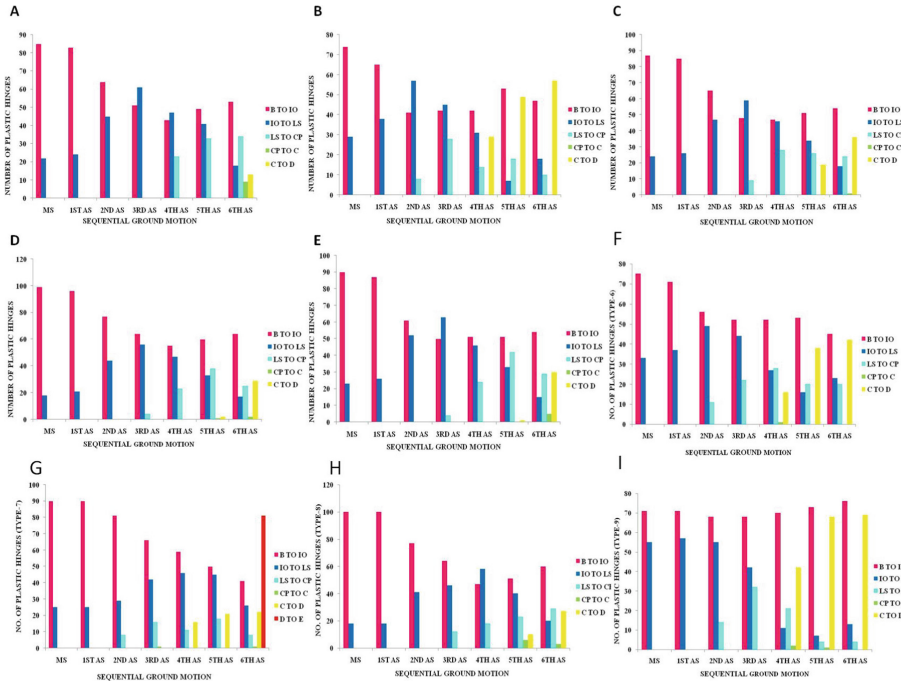


Fig. 17. Number of hinges pattern for A (T_0), B ($T_{1,1}$), C ($T_{1,2}$), D ($T_{1,3}$) and E ($T_{1,4}$), F ($T_{2,1}$), G ($T_{2,2}$), H ($T_{2,3}$), I ($T_{2,4}$) for case 3.

5 Conclusion

From the response of the regular frame and the frames obtained by incorporating two identical stiffness irregularities at different levels of storey subjected to episodes consist of main shocks of PGA 0.36g, 0.4g, and 0.45g and six aftershocks with scaled PGA of 0.66 PGAs of the main shocks, following conclusions are drawn.

- The frames survive under the episode of 0.36g PGA and severity of the damage lessens if the irregularity in a storey is shifted from bottom storey to top storey.
- The frames with stiffness reduced to 43% in first, second, mid-height and top storeys survive all the aftershocks of 0.4g PGA episode. On the other hand, the frames with stiffness reduced to 65% in the top and at mid-height storey, survive with 0.4g PGA episode but intend to collapse earlier during aftershock when the irregularity is with second storey than with first storey.
- With 43% irregularity the severity of the state of damage increases if the irregularity is shifted from top storey to first storey and the frame with higher stiffness irregularity in topmost storey fails earlier than the frame with lower stiffness irregularity in the lowest storey under the episode of 0.45g PGA.
- Post each aftershock residual displacement accumulation is slower in regular frames with lower PGAs episode as compared to the irregular ones, owing to which the

former has higher chances of survival. Moreover, the irregular buildings with stiffness irregularity in the bottom part of the frame tend to have higher accumulation in the residual displacement as compared to those that have irregularities introduced the top parts of the frames. Maximum residual storey drift follows a similar trend.

References

- Ahmadi, E., Alam, M., Anas, S.M.: Blast performance of RCC slab and influence of Its design parameters. In: Kolathayar, S., Ghosh, C., Adhikari, B.R., Pal, I., Mondal, A. (eds.) Resilient Infrastructure, LNCE, vol. 202, pp. 389–402. Springer, Singapore (2021). https://doi.org/10.1007/978-981-16-6978-1_31
- Anas, S.M., Alam, M., Umair, M.: Performance of one-way concrete slabs reinforced with Conventional and polymer re-bars under air-blast loading. In: Chandrasekaran, S., Kumar, S., Madhuri, S. (eds.) Recent Advances in Structural Engineering. LNCE, vol. 135, pp. 171–191. Springer, Singapore (2020a). https://doi.org/10.1007/978-981-33-6389-2_18
- Anas, S.M., Alam, M., Umair, M.: Performance of one-way composite reinforced concrete slabs under explosive-induced blast loading. In: IOP Conference Series: Earth and Environmental Science. 1st International Conference on Energetics, Civil and Agricultural Engineering 2020, Tashkent, Uzbekistan, vol. 614 (2020b). <https://doi.org/10.1088/1755-1315/614/1/012094>
- Anas, S.M., Ansari, Md.I., Alam, M.: Performance of masonry heritage building under air-blast pressure without and with ground shock. Aust. J. Struct. Eng. **21**(4), 329–344 (2020c). <https://doi.org/10.1080/13287982.2020.1842581>
- Anas, S.M., Ansari, Md.I., Alam, M.: A study on existing masonry heritage building to explosive-induced blast loading and its response. Int. J. Struct. Eng. **11**(4), 387–412 (2021a). <https://doi.org/10.1504/IJSTRUCTE.2021.118065>
- Anas, S.M., Alam, M., Umair, M.: Experimental and numerical investigations on performance of reinforced concrete slabs under explosive-induced air-blast loading: a state-of-the-art review. Structures **31**, 428–461 (2021b). <https://doi.org/10.1016/j.istruc.2021.01.102>
- Anas, S.M., Alam, M.: Air-blast response of free-standing: (1) Unreinforced brick masonry wall, (2) Cavity RC wall, (3) RC walls with (i) Bricks, (ii) Sand, in the cavity: a macro-modeling approach. In: Marano, G.C., Ray Chaudhuri, S., Unni Kartha, G., Kavitha, P.E., Prasad, R., Achison, R.J. (eds.) Proceedings of SECON'21. SECON 2021. LNCE, vol. 171, pp. 921–930. Springer, Cham (2021c). https://doi.org/10.1007/978-3-030-80312-4_78
- Anas, S.M., Alam, M.: Comparison of existing empirical equations for blast peak positive overpressure from spherical free air and hemispherical surface bursts. Iran. J. Sci. Technol. Trans. Civ. Eng. **46**, 965–984 (2021d). <https://doi.org/10.1007/s40996-021-00718-4>
- Anas, S.M., Alam, M., Umair, M.: Performance of on-ground double-roof RCC shelter with energy absorption layers under close-in air-blast loading. Asian J. Civ. Eng. **22**, 1525–1549 (2021e). <https://doi.org/10.1007/s42107-021-00395-8>
- Anas, S.M., Alam, M., Umair, M.: Air-blast and ground shockwave parameters, shallow underground blasting, on the ground and buried shallow underground blast-resistant shelters: a review. Int. J. Prot. Struct. **13**(1), 99–139 (2021f). <https://doi.org/10.1177%2F20414196211048910>
- Anas, S.M., Alam, M., Umair, M.: Out-of-plane response of clay brick unreinforced and strengthened masonry walls under explosive-induced air-blast loading. In: Kolathayar, S., Ghosh, C., Adhikari, B.R., Pal, I., Mondal, A. (eds.) Resilient Infrastructure. LNCE, vol. 202, pp. 477–491. Springer, Singapore (2021g). https://doi.org/10.1007/978-981-16-6978-1_37

- Anas, S.M., Alam, M., Umair, M.: Influence of charge locations on close-in air-blast response of pre-tensioned concrete U-girder. In: Kolathayar, S., Ghosh, C., Adhikari, B.R., Pal, I., Mondal, A. (eds.) Resilient Infrastructure. LNCE, vol. 202, pp. 513–527. Springer, Singapore (2021h). https://doi.org/10.1007/978-981-16-6978-1_40
- Anas, S.M., Alam, M.: Performance of simply supported concrete beams reinforced with high-strength polymer re-bars under blast-induced impulsive loading. *Int. J. Struct. Eng.* **12**(1), 62–76 (2022a). <https://doi.org/10.1504/IJSTRUCTE.2022.119289>
- Anas, S.M., Alam, M.: Performance of brick-filled reinforced concrete composite wall strengthened with C-FRP laminate(s) under blast loading. *Mater. Today Proc.* (2022b). <https://doi.org/10.1016/j.matpr.2022.03.162>
- Anas, S.M., Alam, M.: Role of shear reinforcements on the punching shear resistance of two-way RC slab subjected to impact loading. *Mater. Today Proc.* (2022c, in press)
- Anas, S.M., Shariq, M., Alam, M.: Performance of axially loaded square RC columns with single/double confinement layer(s) and strengthened with C-FRP wrapping under close-in blast. *Mater. Today Proc.* **58**, 1128 (2022a). <https://doi.org/10.1016/j.matpr.2022.01.275>
- Anas, S.M., Alam, M., Umair, M.: Strengthening of braced unreinforced brick masonry wall with (i) C-FRP wrapping, and (ii) Steel angle-strip system under blast loading. *Mater. Today Proc.* **58**, 1181 (2022b). <https://doi.org/10.1016/j.matpr.2022.01.335>
- Anas, S.M., Alam, M., Umair, M.: Effect of design strength parameters of conventional two-way singly reinforced concrete slab under concentric impact loading. *Mater. Today Proc.* (2022c). <https://doi.org/10.1016/j.matpr.2022.02.441>
- Anas, S.M., Alam, M., Umair, M.: Performance based strengthening with concrete protective coatings on braced unreinforced masonry wall subjected to close-in explosion. *Mater. Today Proc.* (2022d). <https://doi.org/10.1016/j.matpr.2022.04.206>
- Anas, S.M., Alam, M., Shariq, M.: Damage response of conventionally reinforced two-way spanning concrete slab under eccentric impacting drop weight loading. *Defence Technol.* (2022e). <https://doi.org/10.1016/j.dt.2022.04.011>
- Anas, S.M., Shariq, M., Alam, M., Umair, M.: Evaluation of critical damage location of contact blast on conventionally reinforced one-way square concrete slab applying CEL-FEM blast modeling technique. *Int. J. Prot. Struct.* (2022f). <https://doi.org/10.1177%2F20414196221095251>
- Anas, S.M., Alam, M., Umair, M.: Performance of (1) concrete-filled double-skin steel tube with and without core concrete, and (2) concrete-filled steel tubular axially loaded composite columns under close-in blast. *Int. J. Prot. Struct.* (2022g). <https://doi.org/10.1177%2F20414196221104143>
- Anas, S.M., Alam, M., Shariq, M.: Behavior of two-way RC slab with different reinforcement orientation layouts of tension steel under drop load impact. *Mater. Today Proc.* (2022h, in press)
- Anas, S.M., Alam, M., Umair, M.: Air-blast response of axially loaded clay brick masonry walls with and without reinforced concrete core. In: Fonseca de Oliveira Correia, J.A., et al. (eds.) ASMA 2021, Advances in Structural Mechanics and Applications, STIN 19, pp. 1–18 (2022i). https://doi.org/10.1007/978-3-030-98335-2_4 (2023, in press)
- FEMA-356: Prestandard and Commentary for the Seismic Rehabilitation of Buildings Washington DC: Federal Emergency Management Agency (2000)
- Indian Standard, IS 456: Indian standard plain and reinforced concrete - code of practice. Bureau of Indian Standards, New Delhi, India (2002a)
- Indian Standard, IS 1893: Criteria for earthquake resistance design of structures, Part-I. Bureau of Indian Standards, New Delhi, India (2002b)
- Indian Standard, IS 1893: Criteria for earthquake resistance design of structures, Part-I. Bureau of Indian Standards, New Delhi, India (2016)
- Faisal, A., Majid, T.A., Hatzigeorgiou, G.D.: Investigation of story ductility demands of inelastic concrete frames subjected to repeated earthquakes. *Soil Dyn. Earthq. Eng.* **44**, 42–53 (2013)

- Goda, K.: Nonlinear response potential of mainshock–aftershock sequences from Japanese earthquakes. *Bull. Seismol. Soc. Am.* **102**(5), 2139–2156 (2012)
- Hatzigeorgiou, G.: Ductility demands control under repeated earthquakes using appropriate force reduction factors. *J. Earthq. Tsunami* **4**(03), 231–250 (2010)
- Hatzivassiliou, M., Hatzigeorgiou, G.D.: Seismic sequence effects on three-dimensional reinforced concrete buildings. *Soil Dyn. Earthq. Eng.* **72**, 77–88 (2015)
- Hosseinpour, F., Abdelnaby, A.: Fragility curves for RC frames under multiple earthquakes. *Soil Dyn. Earthq. Eng.* **98**, 222–234 (2017)
- Loulelis, D., Hatzigeorgiou, G., Beskos, D.: Moment resisting steel frames under repeated earthquakes. *Earthquake and Structures* **3**(3–4), 231–248 (2012)
- Mander, J.B., Priestley, M.J., Park, R.: Theoretical stress-strain model for confined concrete. *J. Struct. Eng.* **114**(8), 1804–1826 (1988)
- Oygun, R., Toros, C., Abdelnaby, A.E.: Seismic behavior of irregular reinforced-concrete structures under multiple earthquake excitations. *Soil Dyn. Earthq. Eng.* **104**, 15–32 (2018)
- Parekar, S.D., Datta, D.: Seismic behaviour of stiffness irregular steel frames under mainshock–aftershock. *Asian J. Civ. Eng.* **21**(5), 857–870 (2020). <https://doi.org/10.1007/s42107-020-00245-z>
- Raghunandan, M., Liel, A.B., Luco, N.: Aftershock collapse vulnerability assessment of reinforced concrete frame structures. *Earthq. Eng. Struct. Dyn.* **44**(3), 419–439 (2015)
- SAP2000: S.I. “Analysis reference manual.” Computer and Structures Inc., Berkeley (2016)
- Scott, B., Park, R., Priestley, M.J.N.: Stress–strain behavior of concrete confined by overlapping hoops at and high strain rates. *J. Am. Concr. Insti.* **79**, 13–27 (1982)
- SeismoSoft: SeismoMatch v.5.1.0 (2020). www.seismosoft.com
- Shariq M, Alam M, Husain A, and Anas S M (2022), “Jacketing with steel angle sections and wide battens of RC column and its influence on blast performance. *Asian J. Civ. Eng.* **58**, 487 (2022). <https://doi.org/10.1007/s42107-022-00437-9>
- Tahzeeb, R., Alam, M., Mudassir, S.M.: A comparative performance of columns: reinforced concrete, composite, and composite with partial C-FRP wrapping under contact blast. *Mater. Today Proc.* (2022a). <https://doi.org/10.1016/j.matpr.2022.03.367>
- Tahzeeb, R., Alam, M., Mudassir, S.M.: Performance of composite and tubular columns under close-in blast loading: A comparative numerical study. *Mater. Today Proc.* (2022b). <https://doi.org/10.1016/j.matpr.2022.04.587>
- Tahzeeb, R., Alam, M., Mudassir, S.M.: Effect of transverse circular and helical reinforcements on the performance of circular RC column under high explosive loading. *Mater. Today Proc.* (2022c). <https://doi.org/10.1016/j.matpr.2022.04.676>
- Takeda, T., Sozen, M.A., Nielsen, N.N.: Reinforced concrete response to simulated earthquakes. *J. Struct. Div.* **96**(12), 2557–2573 (1970)
- Ul Ain, Q., Alam, M., Anas, S.M.: Behavior of ordinary load-bearing masonry structure under distant large explosion, Beirut scenario. In: Kolathayar, S., Ghosh, C., Adhikari, B.R., Pal, I., Mondal, A. (eds.) *Resilient Infrastructure*, LNCE, vol. 202, pp. 239–253. Springer, Singapore (2022). https://doi.org/10.1007/978-981-16-6978-1_19
- Ul Ain, Q., Alam, M., Anas, S.M.: Response of two-way RCC slab with unconventionally placed reinforcements under contact blast loading. In: Fonseca de Oliveira Correia, J.A., et al. (eds.) *ASMA 2021, Advances in Structural Mechanics and Applications*, STIN 19, pp. 1–18 (2022). https://doi.org/10.1007/978-3-031-04793-0_17 (2023, in press)